Sua Pan surface bidirectional reflectance: A case study to evaluate the effect of atmospheric correction on the surface products of the Multi-angle Imaging SpectroRadiometer (MISR) during SAFARI 2000

Wedad A. Abdou, Stuart H. Pilorz, Mark C. Helmlinger, James E. Conel, David J. Diner, Carol J. Bruegge, and John V. Martonchik

Jet Propulsion Laboratory, California Institute of Technology, Pasadena, CA 91109.

Charles K. Gatebe and Michael D. King

University of Maryland, Baltimore county,
NASA/GSFC, Greenbelt, MD 20771.

Peter V. Hobbs

Department of Atmospheric Sciences
University of Washington, Seattle, WA 98195.

Abstract: The Southern Africa Regional Science Initiative (SAFARI 2000) dry season campaign was carried out during August and September 2000 at the peak of biomass burning. The intensive ground-based and airborne measurements in this campaign provided a unique opportunity to examine the surface products of the Multi-angle Imaging SpectroRadiometer (MISR), aboard NASA's EOS Terra platform. The MISR validation team participated with a suite of ground-based instruments, including the Portable Apparatus for Rapid Acquisition of Bidirectional Observations of Land and Atmosphere (PARABOLA III) to measure surface bidirectional reflectance factors (BRF). A participating airborne sensor was the Cloud Absorption Radiometer (CAR) flown onboard the University of Washington's Convair-580 research aircraft. In the absence of clouds, the CAR observations provide measurements of the surface BRF. This paper presents a validation case study of MISR surface products where its BRF measurements at Sua Pan, Botswana, during the SAFARI campaign, are compared with those coincidently evaluated on the ground and from the air, using the PARABOLA and CAR observations, respectively. Since atmospheric correction is critical to the BRF retrieval process, two data sets are used in this study: one was collected under clear atmospheric conditions on August 27, and the other, on September 3, exhibited hazy conditions due to several grass fires near Sua Pan. The presence of haze and smoke on September 3 provided a case study to evaluate the effect of atmospheric correction on MISR surface products. Two surface types were considered in the analyses: the bright desert-like surface of the Pan and the dark grassland that surrounds it. The results show that, for the grassland surface type, the BRF values retrieved from MISR in the blue, green and red channels, on both days are within 5% to 10% with those obtained from CAR and PARABOLA data. In the back scattering nir channels, however, MISR BRF values are overestimated in comparison with airborne and ground measurements. For the bright desert-like pan surface, better agreement was found in all channels on the clear day (558 nm optical depth of 0.08) but only in the forward scattering on the hazy day (558 nm optical depth of 0.72). On this day, the MISR BRFs in the back scattering viewing cameras are darker than those obtained from either the CAR or the PARABOLA data. A comparison of the aerosol optical depth retrieved from MISR to those obtained from three independent ground measurements suggest that small uncertainties in the MISR aerosol and surface retrieval process become magnified at large optical depths.

1. Introduction

The Multi-angle Imaging SpectroRadiometer (MISR) was launched on December 18, 1999, into a 705-km sun-synchronous Earth orbit aboard the Earth Observing System (EOS) Terra spacecraft. The MISR instrument [Diner et al., 1998] has nine Charge Coupled Device (CCD) push broom cameras that view the Earth's surface in four spectral bands centered at 446, 558, 672 and 866 nm, and at angles of 0^o (An), 26.1^o (Af, Aa), 45.6^o (Bf, Ba), 60.0^o (Cf, Ca) and 70.5^o (Df, Da), relative to nadir, in both forward (f) and aft (a) along the direction of flight, where the notations in parentheses are shorthand names for the cameras. The major science goal of EOS and of MISR is to provide well-calibrated and validated measurements of key parameters that are crucial to the long-term assessment of temporal variations in the Earth's radiation budget especially those due to clouds, aerosols, and land-surface albedo. The MISR data products provide information on atmospheric aerosol (e.g., optical depth, column-averaged particle size distribution, etc.) the surface bidirectional reflectance factor (BRF) and the hemispherical directional reflectance factor

(HDRF). The BRF, an inherent property of the surface that characterizes its directional reflectance anisotropy, is defined as the ratio of the radiance reflected by the target surface in a specific direction to that reflected in the same direction by a perfectly diffuse (Lambertian) surface illuminated by the same collimated beam (i.e., direct illumination only). The HDRF characterizes the angular reflectance properties of the surface under ambient illumination (i.e., in presence of diffuse illumination), hence its dependency on atmospheric conditions. The integration of the BRF and the HDRF over view angles provides the directional-hemispherical reflectance (DHR) and the bihemispherical reflectance (BHR). The latter is commonly known as the albedo, while the DHR is sometimes referred to as the black-sky albedo (i.e., the albedo in the special case of illumination from a collimated beam - detailed definitions of these surface parameters are given by Martonchik et al. [2000] and Nicodemus et al., [1977]).

Proper knowledge of surface albedos is crucial to the understanding of the radiative processes that govern the Sun-Earth system and to the assessment of the Earth's radiation budget. It is, therefore, of interest to ensure accurate surface measurements from satellite instruments, such as MISR. This work describes a validation case study of MISR surface products, specifically the BRF, by comparing their values as retrieved from MISR to those determined simultaneously, but independently, from other measurements. Because atmospheric correction is crucial to the MISR surface retrieval process, it is important to examine MISR aerosol products, mainly the aerosol optical depth and type, and their effects on the accuracy of the retrieved BRF.

The Southern Africa Regional Science Initiative (SAFARI 2000) dry season field study, carried out in the year 2000 during August and September, provided an opportunity to perform this validation experiment. In that campaign a wide range of intensive ground- and airborne-based measurements of the surface and atmosphere properties were coordinated during Terra overpasses [Swap et al., 2002 and King et al., 2003]. Several of these ground and aircraft measurements are employed in this study.

2. MISR surface retrieval strategy

The MISR surface retrieval algorithm involves inversion of the solution to the radiative transfer equation [Chandrasekhar, 1960] to convert the observed top-of-atmosphere (TOA) radiance (normalized to an Earth-Sun distance of 1 AU and corrected to ozone absorption) to surface parameters. This approach requires knowledge of the atmosphere's reflective and transmissive properties, both of which are functions of aerosol optical depth and type. These atmospheric characteristics are determined in the MISR aerosol retrieval process, based on a principal component analysis of the TOA radiance [Martonchik et al., 1998a; Martonchik et al., 2002a]. The technique does not require knowledge of the absolute surface reflectance or its spectral characteristics but does require sufficient scene spatial contrast at various MISR view angles. An essential component of the aerosol retrieval process is a look-up table (LUT) of path radiances simulated for a preselected set of aerosol mixtures that are commonly found in the atmosphere. Once the atmospheric properties are determined, the strategy is to retrieve the surface HDRF first and then proceed to obtain the BRF. Determination of the HDRF involves removal of the effects of atmospheric path radiance and the upward direct and diffuse transmission effects on the surface reflected radiance. The surface BRF is then derived from the HDRF by removing the effects of downward diffuse sunlight

and assuming a parameterized BRF [Rahman et al., 1993]. The LUT is central to this atmospheric correction process and the selected aerosol mixtures greatly impact the accuracy of retrieving the aerosol and, consequently, the surface products. The BRF measurements at SAFARI 2000 present an opportunity to evaluate the effect of the above atmospheric correction on MISR surface retrieval. Details of MISR aerosol and surface retrieval algorithms are beyond the scope of this work and could be found in Martonchik et al., [1998a,b].

3. Surface BRF measurements at SAFARI 2000.

The SAFARI campaign covered multiple sites in southern Africa. This work focuses only on the data collected at Sua Pan, Botswana (20.6^o S, 26.1^o E). Sua Pan, one of the salt pan in northeastern Botswana, is about 3500 km^2 of desert-like surface surrounded by grasslands. The pan surface is mainly a semi-hard clay mud with varying degrees of water saturation (the entire pan surface floods seasonally) in its upper layers and a thin salt crust on top. Tracks are easily made, due to people and vehicles moving on the pan, exposing relatively darker layers just beneath the top surface. The pan surface appears inhomogenous at the small scale of ~1 m but appears homogeneous at larger scale. Figure 1 shows MISR images of the Sua pan site from space on the clear day of August 27 (a) and the hazy day of September 3, 2000 (b).

This study compares the BRF retrieved from MISR data at Sua Pan during the SAFARI 2000 campaign with those measured simultaneously, but independently, on the ground and from an aircraft. The three independent measurements, cover two types of surfaces: 1) the bright desert-like surface of the pan, and 2) the dark dry grassland that surrounds the pan. Figure 1a is zoomed in to show the locations of the field campaign, defined by the rectangular box and the “x” marks. Details of these measurements are described next.

3.1 MISR measurements

Two MISR data sets obtained at Sua Pan, on August 27 and September 3, 2000, are selected for this study (it is important to note that the MISR data used here are the publicly available MISR surface and aerosol products version F04_0015 and F07_0015, respectively.) On these two days, at ~0852 UTC (~1052 local time), MISR passed over Sua Pan, in orbits 3684 (path 172, block 107) and 3786 (path 173, block 107), respectively. Tables 1 and 2 show MISR viewing geometries on both days. The MISR images of Sua Pan indicate clear atmospheric conditions on August 27 (Figure 1a), and thick haze and smoke on September 3, due to wild and man-made grass fires that erupted earlier at several spots near Sua Pan (Figure 1b). This large difference in aerosol loading provides an opportunity to evaluate the effect of the MISR atmospheric correction process on retrieving the surface parameters.

MISR BRF values, at each of the nine view angles, is averaged over a group of 2 x 2 (1.1 km) pixels that cover the ground locations marked with “x” in Figure 1a. The locations represent the bright desert-like and the grassland surface types. Ground and airborne data were collected at these two locations during the campaign as discussed next.

3.2 Ground measurements

The MISR validation team was present at Sua Pan from August 24 to September 4, 2000, and made daily measurements of the surface directional reflectance using the Portable Apparatus for Rapid Acquisition of Bidirectional Observations of Land and Atmosphere (PARABOLA) version III [Bruegge et al., 2000]. The third-generation sphere-scanning radiometer built by Sensit Corporation (Mayville, ND) represents a substantial revision in design and capability over the first version of this instrument [Deering and Leone,1986].

PARABOLA III consists of two separate sensor heads mounted at opposite ends of a center-suspended horizontal scanning arm that rotates continuously through 360° about a vertical axis. Each sensor head contains the detector assemblies for four of eight channels (444, 551, 650, 860, 944, 1028. 1650 and 400-700 nm). Each individual head scans synchronously with the other from zenith to nadir in vertical angle. The combined synchronized motion of the heads about both axes generates a steppers pattern of 5° circular full apex angle overlapping fields of view of sky hemisphere, and a series of 5° ellipsoidal pixels on the ground that increase in length from nadir to horizon (~10 cm in the nadir to ~10 meters at ~80^{o}, when the PARABOLA is set ~2 m above ground). An entire scan of both sky and ground hemispheres generates 2664 (= 37 x 72) pixels in about 3 minutes including downloading to memory. A Spectralon panel, placed in the south-west corner of the PARABOLA nadir field of view, provides the perfect Lambertian standard reference required for the BRF calculations (based on the definition given in the introduction). In practice, the Spectralon reflectance deviates slightly from that of a perfect lambertian surface and a correction factor, equal to the Spectralon BRF at the specific viewing and illuminating geometry, is required to correct for its nonmetal reflectance properties. A database for the Spectralon BRF is available from Bruegge et al. [2001] to determine the required correction factor. Details of the PARABOLA III measurements and calibration procedures are described by Bruegge et al. [2000].

The surface BRF is retrieved from the PARABOLA data using a methodology developed by Martonchik, [1994]. The technique requires measurements, at the same location, over a range of solar angles, preferably from sunrise to noon or from noon to sunset. The data obtained during the clear day of August 27 and the hazy day of September 3 were processed, as described by Abdou et al. [2000] and examples of the BRF retrieved on August 27 are illustrated in Figure 2. This polar plot shows an almost diffusely reflecting surface, that exhibit no strong angular signatures. The surface BRF increases with wavelengths and is enhanced in the back scattering directions.

For meaningful comparison with MISR, the PRABOLA data must represent the reflectance over an area equal in size to that covered by MISR footprints (1.1 x 1.1 km/ pixel). To make sure of that, a portable spectrometer was used to evaluate the average reflectance of the pan surface within this area. The portable spectrometer, manufactured by Analytical Spectral Devices, Inc. (ASD, Boulder, CO), provides rapid estimates of the surface spectral HDRF (in the nadir direction) between 350 and 2500 nm at an average spectral resolution of ~10 nm. The ASD sampling technique is to alternately measure the radiance reflected from the target surface and that reflected from a reference Lambertian surface, in this case the Spectralon panel and the surface HDRF is determined by the ratio of the two radiances. The correction factor, mentioned above, is applied to

account for the deviation of the Spectralon reflectance from Lambertian. The ASD measurements were made at 20 points along representative transacts laid out over the area surrounding the PARABOLA location. The few seconds sampling time allowed these measurements to be made without significant changes in the illumination or atmospheric conditions during the Terra overpass time. The ASD data were collected at various locations on the pan and on the grassland (within the rectangle shown in Figure 1a) on August 24, 25 27 and 30, 2000 and on September 3, 2000, under cloud-free conditions and close to the Terra satellite overpass times. Figure 3 illustrates the range of these measurements. The ASD data obtained at various points within the footprint of the MISR 2 x 2 pixels were averaged and were used to normalize the PARABOLA BRF in the nadir. A Global Positioning System (GPS) was used to geolocated the ground field measurements to help minimize errors in collocating various data. The PARABOLA together with the ASD measurements provide the BRF within ~ 2 to 3% accuracy at solar and view angles smaller than ~45^o and within ~8% at more oblique angles {Abdou et al., 2000]. In the present analyses, an upper limit of 10% uncertainty is assumed. For more on the measurements see field engineers reports at: www-misr.jpl.nasa.gov/mission/valwork/valwork/val_reports/000813_safari.

3.3 Airborne measurements

BRF measurements were made during the MISR overpass with the Cloud Absorption Radiometer (CAR) that flew aboard the University of Washington Convair-580 research aircraft over Sua Pan on September 3 [Getabe et al., 2003]. The CAR is an airborne multi spectral scanning radiometer developed at Goddard Space Flight Center originally for the study of spectral cloud absorption [King et al., 1986]. The instrument is designed to scan the sky downwelling and the ground upwelling radiances from zenith to nadir in 1^o field of view in 14 spectral channels (340-2300 nm). Under cloud-free conditions, the multiangle viewing geometry of the CAR allows determination of the directional reflectance properties of terrestrial surfaces [Tsay et al., 1998; Soulen et al., 2000; Gatebe et al., 2001]. As the Convair-580 flew in ~3 km circles at 600 m altitude above the Sua Pan, the CAR made several complete orbital measurements that extended from 0949 to 1000 UTC at a solar zenith angle of ~28.5^o. At 600 m altitude, the resolution of the CAR is ~ 10 m at nadir and ~ 270 m at 80^o view angle. The surface BRF was retrieved from the CAR measurements after applying an atmospheric correction to remove the radiances scattered by the ambient atmosphere [Gatebe et al., 2003].

4. Results and discussion

The PARABOLA and CAR BRFs were available every 5^o and 1^o, respectively, in both zenith and relative azimuth angles. These data were linearly interpolated to MISR viewing geometries (Tables 1 and 2) and wavelengths and compared with the values retrieved from MISR data on August 27 and September 3, as shown in Figures 4 and 5, respectively. There were no PARABOLA data available for the grassland on either days and no CAR data available on August 27. The data were collocated at the two sites (marked with “X” in Figure 1a) that characterize the bright desert-like surface of the pan and the dry grassland that surrounds it. The CAR data obtained on

September 3, were corrected for the difference in the solar angle of the measurements by multiplying the CAR data by the ratio of the two solar angles.

Figure 4 shows that on the clear day of August 27, the BRFs retrieved from MISR data for the bright desert-like surface agree within 0.01 to 0.05, in absolute value, with the ground-based BRF in all of the channels except in the two blue back scattering channels, at 70.6^{o} and 60.5^{o}, where the agreement is ~0.1. MISR accuracy requirements for the BRF retrievals are the largest of $\pm$0.03 or 10%. Agreements between MISR and the PARABOLA measurements in the nadir and near nadir channels are better than 0.025.

Figure 5 illustrates the data collected on the hazy day, September 3. On that day, CAR data were available for the bright desert and grassland surface types. For the bright desert-like surface of the pan, MISR BRF values retrieved in the forward scattering channels agree within 0.01 to 0.05, in absolute values, with the corresponding airborne and ground measurements. In the back scattering direction, however, MISR BRFs are underestimated relative to the CAR and PARABOLA data. The disagreements, as shown in Figure 5, are maximum at the most oblique cameras, in the blue band. A similar pattern also appears between the CAR and PARABOLA BRFs. Figure 5 also illustrates the comparison between the BRF values retrieved on the same day from MISR and the CAR instrument at the grassland site. The agreements in this case are mostly within 0.01.

The above results show that MISR BRFs are mostly in reasonable agreements with the ground and airborne field measurements, except for the bright surface on the hazy day. This suggests the atmospheric correction process as one likely source of the discrepancy. The excellent agreement between MISR's and CAR's BRF values for the dark grassland site on the same hazy day appears inconsistent with this conclusion. However, the two other known sources of errors do not explain the discrepancy shown in Figure 5. These are the uncertainty in co-locating and scaling the data from the three instruments, and the MISR radiometric calibration. The latter, validated to be within ~4% [Bruegge et al., 2002] for all spectral bands, does not explain errors in only some of the cameras and is, therefore, excluded as a possible source for the above discrepancy.

The effect of co-locating and scaling the data is expected to introduce some errors due to the large difference between MISR resolution and those of CAR and PARABOLA, especially in the most oblique angles and when the surface exhibits large differences in brightness as shown in Figure 3. However, using the numerous ASD data at various locations on the pan, and the field GPS data that accompanied the ground and aircraft measurements, and with a geo-registration of MISR images better than 1 pixel [Jovanovic et al., 2002], the co-location and scaling of the data was a straightforward process. Also, the 10% error bars cover the variability in brightness of the pan surface and, except for the bacscattering channels in the case of the bright surface, most of the disagreements are within these error bars. For the dark grassland surface, as shown in Figure 3, the ASD data show smaller variation in surface reflectance indicating a more homogeneous surface and, therefore, smaller error bars.

5. Evaluation of MISR atmospheric correction process.

The atmospheric correction process remains the most plausible source of the discrepancy shown in Figure 5. In this study, it is useful to make use of the aerosol measurements that were available during the campaign in order to evaluate the effect of MISR atmospheric correction on the retrieval of the Sua pan BRF during the SAFARI experiment. This is done by examining MISR aerosol products and comparing them with some of those made in the field on the ground and from the Convair-580.

5.1. Aerosol field measurements

The MISR team made several measurements of the aerosol optical depth using auto tracking Reagan sun-radiometers. Two of these radiometers were used to measure the incident solar irradiance in 10 spectral channels in the range 380 to 1030 nm. These instruments were calibrated (zero airmass instrument response determined) using the well known Langley technique [Shaw et al., 1973]. The Rayleigh scattering optical depth, required by this technique, is calculated from field measurements of atmospheric pressure. The residual optical depth consisting of the total instantaneous optical depth minus Rayleigh component is the starting point for simultaneous retrieval of the aerosol and ozone components using the procedure developed by [Flittner et al., 1993]. Figure 6 illustrates the aerosol optical depth obtained from the sun photometers' measurements on August 27 and September 3. The data on September 3 indicate the thick haze and smoke that were present on that day. The CIMEL Sunphotometer (manufactured by Cimel Electronique, France) was also used to measure light scattering in the solar aureole, as well as in the almucantar and the principal plane. The CIMEL data provide the atmospheric optical depth, shown also in Figure 6, but they are used, in addition, to determine the aerosol phase function, single scattering albedo, and particle size distribution using the retrieval algorithm described by Dubovik and King [2000]. The CIMEL data on September 3 indicate a relatively absorbing aerosol with a single scattering albedo, ω_0, of 0.88 and a complex refractive index of 1.44-0.01i in the MISR green band. The retrieved volume particle size distribution, shown in Figure 7a, has three modes with characteristic radii of about 0.1, 1.0 and 6.0 μm. No results were available for August 27, but those available on August 28 show a size distribution similar to the one obtained for September 3. The CIMEL results obtained for the SAFARI campaign sites are posted on the AErosol RObotic NETwork (AERONET) website at: aeronet.gsfc.nasa.gov [Holben et al., 1998].

Additionally, an integrating 3-wavelength nephelometer and a Particle Measurement System (PMS) model PCASP-100X were aboard the Convair-580 to measure the vertical profiles of the aerosol light scattering coefficient and particle size distribution over Sua Pan on September 3 **[**Hobbs, 2003**].** Figure 7b compares the in situ particle size distribution with that inverted from the CIMEL ground measurements (shown in Figure 7a) after converting the latter to column number density particle size distribution (using an aerosol column length of ~3 km). The in situ particle size distribution measurements indicate a well mixed aerosol with at least two modes, one at ~0.1 μm and the other at ~1.0 μm radius. It should be noted that the in situ measurements are sensitive only to particle size in the range 0.06 to 1.5 μm in radius, while the AERONET inversion is sensitive to particles size from 0.05 to 15 μm. Within these radii range of overlapping sensitivity, the two independent measurements, shown in Figure 7b, are reasonably consistent. Also, the vertical profiles of the aerosol light scattering coefficient was found consistent with that estimated from the AERONET data.

5.2. MISR aerosol measurements

The MISR aerosol retrievals over Sua Pan for August 27 and September 3 are shown in Figure 8. The optical depth values retrieved on both days are underestimated relative to those retrieved in the field. The standard operational algorithm is based on a set of 24 aerosol models (Mixture file version F04_0005) based on 11 pure particles (Kahn et al., 2005). The retrieved aerosols were mixtures of particles that are smaller and, therefore, have larger phase functions, than those retrieved from the airborne and ground measurements, resulting in an underestimation of the retrieved optical depths. It was clear from this, and several other independent studies, that the aerosol look-up table requires improvement. The aerosol team at JPL has been conducting research studies with new set of aerosol mixtures to improve the aerosol retrieval process.

A new look-up table [under development at JPL] that is now being introduced for operational retrievals, contains radiances simulated for 74 aerosol models that are based on 21 pure particles. Figure 9 shows a comparison of the optical depth and surface BRF retrieved (in all MISR pixels of block 107 that contains Sua Pan) with the 24 and the 74 mixture sets. The new mixture set results in a general increase in optical depth values while not affecting the surface retrieval significantly. The optical depth retrieved from MISR using the new look-up table are shown in Figure 10. It is clear that the retrieved optical depths are now in better agreement with their corresponding values measured in the field. The retrieved aerosol models for August 27 and September 3 are mixtures of a white particle, with a characteristic radius of 1.0 μm, with an absorbing particle with a characteristic radius of 0.06 μm. The effective radii of these mixtures (~0.12 μm) are relatively smaller than those measured in the field and their effective single scattering albedos are higher and vary from 0.91 to 0.925, depending on the mixing ratios of the white relative to the absorbing particles. The retrieved surface BRF, however, has not changed significantly. The top-of-atmosphere (TOA) radiance expected from such an aerosol model exceeds those from the more absorbing particles that were measured in the field. The retrieval process compensates for the excess radiance, either by retrieving a smaller optical depth or, as the case here, a smaller BRF. Figure 11 compares MISR (TOA) radiances in the green band with those estimated by radiative transfer calculations (using a validated a one-dimentional radiative transfer code that is based on the discrete ordinate matrix operator method of Grant and Hunt (1968]) calculations, using the field measurements of optical depth and surface BRF with the aerosol models retrieved from MISR. The comparison is made for the hazy day, where the aerosol contribution to the TOA radiance is significant. In the case of the dark grassland, the simulated and measured TOA radiances are in good agreement. However, over the bright desert-like surface of the pan, the simulated radiances are much larger in the back scattering direction than those actually observed. This can be explained as due to the enhancement of the aerosol multiple scattering in the presence of a bright surface while the opposite is true in the presence of a dark absorbing surface. The discrepancy is larger in the back scattering direction because the retrieved aerosols are mixtures of relatively smaller particles than those measured in the field. Smaller particles are characterized by relatively larger phase functions in the back scattering direction. The uncertainties in the properties of the retrieved aerosol models, therefore, produce significant effect in case of a bright surface under an optically thick atmosphere. These results are of interest to the community involved in surface properties and characterization. Further work should be done to identify and evaluate more of these cases.

6. Conclusion

This paper describes a case study of MISR BRF retrievals using ground and airborne measurements that were made at Sua Pan, Botswana, during the SAFARI 2000 dry season campaign. Two sets of data, one on a clear day on August 27 and the other on a hazy day on September 3, were selected to examine the effects of atmospheric correction on the MISR surface retrieval process. MISR BRF was evaluated for bright desert-like and dark grassland surfaces. The BRF's retrieved from the MISR data generally have the same angular behavior as those determined from the ground and airborne data, with their absolute values in good agreements with most of the field measurements except on the hazy day at the bright surface. MISR aerosol retrieval was discussed as a possible source of these disagreements. It is evident from the results presented here that, in the case of bright surfaces under optically thick atmospheric conditions, the multiple scattering between aerosol particles and aerosol and surface, may enhance the effect of small uncertainties in the aerosol properties causing significant errors in the surface BRF retrieval. Further work to Isolate and evaluate more of these cases will be most valuable. Also, it is important to repeat this work for cases that envolve heterogeneous surfaces and various degrees of brightness.

7. Acknowledgments. The authors thank B. N. Holben for making the CIMEL data available on the AERONET site. This study was conducted at the Jet Propulsion Laboratory, California Institute of Technology, under contract with NASA (the National Aeronautics and Space Administration). The University of Washington team was supported by NASA and the National Science Foundation (NSF).

8. REFERENCES

Abdou W. A., M. C. Helmlinger, J. E. Conel, C. J. Bruegge, S. H. Pilorz, J. V. Martonchik, and B. J. Gaitley, Ground measurements of surface BRF and HDRF using PASRABOLA III., *J. Geophys. Res.*, **106**, 11,967-11,976, 2000.

Bruegge, C. J., Nadine L. Chrine, Robert R. Ando, David J. Diner, Wedad A. Abdou, Mark C. Helmlinger, Stuart H. Pilorz, and K. Thome, Early Validation of the Multi-Angle Imaging SpectroRadiometer (MISR) Radiometric Scale, *IEEE Transaction on Geoscience and Remote Sensing*, **40**, No 7, July 2002.

Bruegge, C. J., Nadine L. Chrine, and David Haner, A Spectralon BRF data base for MISR calibration applications, *Rem. Sens. Environ.*, **76**, 354-366, 2001.

Bruegge, C. J., M. C. Helmlinger, J. E. Conel, B. J. Gaitley, and W. A. Abdou, PARABOLA III: a shpere-scanning radiometer for field determination of surface anisotropic reflectance functions, *Remote Sens. Rev.*, **19**, 75-94, 2000.

Chandrasekhar, S., *Radiative Transfer*, Dover Publication, Inc., New York, 1960.

Deering, D. W., and P. Leone, A sphere-scanning radiometer for rapid directional measurements of sky and ground radiance, *Remote Sens. Environ*., **19**, 1-24, 1986

Diner, D. J, C. J. Bruegge, J. V. Martonchik, T. P. Ackerman, R. Davies, S. A. W. Gerstl, H. R. Gordon, P.J. Sellers, and J. Clark, J. A. Daniels, E. D. Danielson, V. G. Duval, K. P. Klassen, G. W. Lilienthal, D. I. Nakamoto, R. Pagano, and T. H. Reilly, MISR: A Multi-angle Imaging SpectroRadiometer for geophysical and climatological research from EOS, *IEEE Trans. Geosci. and Remote Sens*., **27**, 200-214, 1989.

Dubovik, O. and M. D. King, A flexible inversion algorithm for retrieval of aerosol optical properties from Sun and sky radiance measurements, *J. Geophys. Res.*, **105**, 20 673-20 696, 2000.

Flittner, D. E., Herman, B. M., Thome, K. J., and Simpson, J. M., Total ozone and aerosol optical depths inferred from radiometric measurements in the Chappuis absorption band, *J. Atmos. Sci.*, **50(8)**, 1113-1121, 1993.

Gatebe, C. K., M. D. King, S. C. Tsay, Q. Ji, G. T. Arnold and J. Y. Li, Sensitivity of off-nadir zenith angles to correlation between visible and near-infrared reflectance for use in remote sensing of aerosol over land, *IEEE Trans. Geosci. Rem. Sens.* **39**, 805-819, 2001.

Gatebe, C. K., M. D. King, S. Platnick, G. T. Arnold, E. F. Vermote, and B. Schmid, Airborne spectral measurements of surface-atmosphere anisotropy for several surface and ecosystem over southern africa, *J. Geophy. Res*., **108** (D13), 8489, doi:10.1029/2002JD002397, 2003.

Grant, I. P. and Hunt, G. E., Solution of radiative transfer problems using the invariant S_n method. *Monthly Notice of the Royal Astronomical Society*, **141**, 27-41, 1968.

Hobbs, P. V., Technical Appendix: An overview of the University of Washington's airborne measurements in the SAFARI 2000 field study in southern Africa, *J. Geophys. Res.*, **108** (D13), 8487, doi:10.1029/2002JD002325, 2003.

Holben, B. N., T. F. Eck, I. Slutsker, D. Tanre, J. P. Buis, A. Setzer, E. Vermote, J. A. Reagan, Y. Kaufman, T. Nakajima, F. Lavenu, I. Jankowiak, and A. Smirnov, AERONET-A federal instrument network and data archive for aerosol characterization, *Rem. Sens. Environ.*, **66**, 1-16, 1998.

Jovanovic, V., M. M. Smyth, J. Zong, R. Ando, and G. W. Bothwell, MISR In-flight camera geometric model Calibration and georectification performance, *IEEE Trans. Geosci. Remote Sens.*, **40**, 1512-1519, 2002.

Kahn, R. A., B. J. Gaitley, J. V. Martonchik, D. J. Diner, K. A. Crean, and B. Holben, MISR global aerosol optical depth validation based on two years of coincident AERONET observations, *J. Geophys. Res.*, **110**, No D10, D10s04, 10.1029/2004JD004706, 2005.

King, M. D., S. Platnick, C. C. Moeller, H. E. Revercomb, and D. A. Chu, Remote sensing of smoke, land and clouds from the NASA ER-2 during SAFARI 2000. *J. Geophys. Res.*, 108, 8502, doi: 10.1029/2002JD003207, 2003.

King, M. D., M. G. Strange, P. Leone, and L. R. Blaine, Multiwavelength scanning radiometer for airborne measurements of scattered radiation within clouds, *J. Atmos. Oceanic. Tech.*, **3**, 513-522, 1986.

Martonchik, J.V., D.J. Diner, K.A. Crean and M.A. Bull, Regional aerosol retrieval results from MISR, *IEEE Trans. Geosci. Remote Sens*., **40**, 1520-1531, 2002a.

Martonchik, J. V., Carol J. Bruegge, and Alan H. Strahler, A review of reflectance nomenclature used in remote sensing, *Rem. Sens. Rev.*, **19**, 9-20, 2000b.

Martonchik, J. V., D. J. Diner, B. Pinty, M. M. Verstrate, R. B. Myneni, Y. Knyazikhin and, H. R. Gordon, Determination of the land and ocean reflective, radiative, and biophysical properties using multiangle imaging, *IEEE Trans. Geosci. Remote Sens.*, **36**, 1266-1281, 1998a.

Martonchik, J. V., D. J. Diner, R. Kahn, M. M. Verstrate, B. Pinty, H. R. Gordon, and T. P. Ackerman, Techniques for the retrieval of aerosol properties over land and ocean using multiangle imaging, *IEEE Trans. Geosci. Remote Sens*., **36**, 1212-1227, 1998b.

Martonchik, J. V., Retrieval of surface directional reflectance properties using ground level multiangle measurements, *Rem. Sens. Environ.*, **50**, 303-316, 1994.

Nicodemus, F. E., J. C. Richmond, J. J. Hsia, I. W. Ginsberg, and T. Limperis, Geometric Considerations and Nomenclature for Reflectance, U. S. A. Department of Commerce/ National Bureau of Standards, *NBS Monograph*, **160**, 1-52, 1977.

Rahman, H., B. Pinty, and M. M. Verstraete, Coupled surface-atmosphere reflectance (CSAR) model 2. Semiempirical surface model usable with NOAA Advanced Very High Resolution Radiometer data, *J. Geophys., Res.*, **98**, 20791-20801, 1993.

Shaw, G.E., J.A. Reagan, and B.M. Herman, Investigations of atmospheric extinction using direct solar radiation measurements made with a multiple wavelength radiometer, *J. App. Meteorol.* **12**, 374-380, 1973.

Soulen, P. F., M. D. King, S. C. Tsay, G. T. Arnold, and J. Y. Li, Airborne spectral measurements of surface anisotropy during the SCAR-A, Kuwait oil fire, and TARFOX experiment, *J. Geophys. Res.*, **105**, 10203-10218, 2000.

Tsay, S. C., M. D. King, G. T. Arnold, and J. Y. Li, Airborne spectral measurements of surface anisotropy during SCAR-B, *J. Geophys. Res*., **103**, 31943-31954, 1998.

Swap, R. J., H. J. Annegarn, J. T. Suttles, J. Haywood, M. C. Helmlinger, C. Hely, P. V. Hobbs, B. N. Holben, J. Ji, M. D. King, T. Landmann, W. Maenhaut, L. Otter, B. Pak, S. J. Piketh, S. Platnick, J. Privette, D. Roy, A.M. Thompson, D.Ward, and R. Yokelson, The Southern African Regional Science Initiative (SAFARI 2000): Overview of the dry-season field campaign, *South African J. of Sci*., **98**, 125-130, 2002.

8. Figure Captions

Figure 1. MISR images of Sua Pan, Botswana, on (a) August 27 and (b) September 3. The rectangular box shown in Figure 1a defines the ground campaign site. The "X" marks the locations of the ground and airborne measurements. The haze shown in (b) is due to smoke from biomass fires that were present near Sua Pan. The relatively clear atmosphere on August 27 was due to the wind conditions, which cleared out the smoke that morning.

Figure 2. A polar plot of the surface BRF retrieved from the PARABOLA measurements at the bright-desert like surface of Sua pan on August 27, 2000, during a Terra overpass. The sun zenith angle for the data in this plot is ~35^{o}. The wavelength (in nm) of the measurements are shown.

Figure 3. The surface HDRF as measured by the ASD instrument on August 27 and September 3 at various locations on the pan surface, within the box shown in Figure 1a, and on the grassland. The HDRF values represent the range of brightness of the pan surface and of the grassland.

Figure 4. A comparison of the BRF retrieved from MISR data at Sua Pan on August 27 with those retrieved on the same day from the ground-based PARABOLA at MISR four wavelengths. The error bars represent the estimated maximum error (10%) in ground measurements.

Figure 5. A comparison of the BRF retrieved from MISR data at Sua Pan on September 3, with those retrieved from the ground-based PARABOLA and the aircraft-based CAR data. The error bars are the estimated maximum error (10%) in ground measurements.

Figure 6. The optical depth values measured by the sun-radiometers at Sua Pan, on August 27 and September 3, during a Terra overpass at 0852 UTC.

Figure 7. (a) The aerosol column particle volume size distribution retrieved (using the Dubovik and King method [2000]) from the CIMEL (AERONET) data at Sua Pan on September 3, and (b) The insitu particle size distribution in $cm^{-3}/\mu m$ (left) measured at three different altitudes by the PMS PCASP-100X aboard the Convair-580. Also shown, for comparison, the aerosol column number density particle size distribution in $cm^{-2}/\mu m$ (right) that is estimated from the data shown in (a) using an aerosol column length of 3 km.

Figure 8. Aerosol optical depth retrieved from MISR data at Sua Pan for (a) the clear day on August 27, and (b) the hazy day on September 3 (b).

Figure 9. Comparison of the surface BRFs (left side panels) and optical depths (right side panels) retrieved from all of MISR's cameras, on both days, using the standard LUT containing 24 aerosol

models (Mixtures file version F04-0005) with those retrieved using a new LUT that contains 74 aerosol models.

Figure 10. As in Figure 8 but with the new 74 aerosol models. With the new LUT MISR retrieved optical depths are closer to the field measurements.

Figure 11. MISR measured radiances above the grassland (a) and the pan surface (b) as compared to those calculated using the corresponding CAR and AERONET measurements of the surface BRF and optical depths, respectively, but the aerosol type retrieved by MISR. The error bars represent an estimated maximum (10%) in the ground surface measurements.

9. Tables.

Table 1: MISR zenith and azimuth (relative to the sun) view angles on August 27, 2000. At overpass time the sun zenith angle wa 37.85^o

Camera	Df	Cf	Bf	Af	An	Aa	Ba	Ca	Da
Zenith	70.6	60.5	46.1	26.7	3.6	26.0	45.4	59.9	70.3
Relative Azimuth	159.3	159.9	161.1	164.6	119.1	30.3	26.7	25.5	25.0

Table 2: MISR Zenith and azimuth (relative to the sun) view angles on September 3, 2000. At overpass time the sun zenith angle was 34.6^o.

Camera	Df	Cf	Bf	Af	An	Aa	Ba	Ca	Da
Zenith	70.4	60.3	46.1	27.4	10.4	28.1	46.5	60.5	70.8
Relative Azimuth	152.6	150.5	146.5	136.0	64.5	2.65	12.7	16.7	19.0

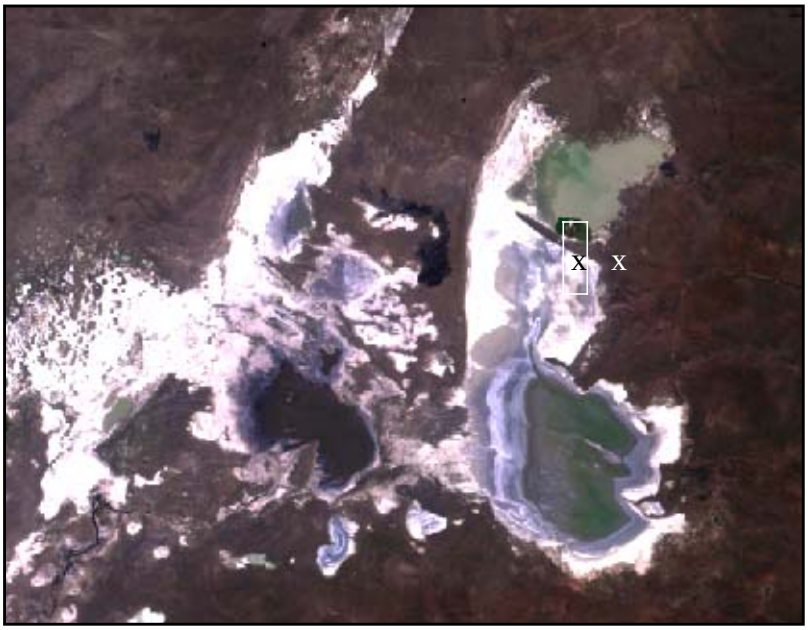

Figure 1a.

Figure 1b.

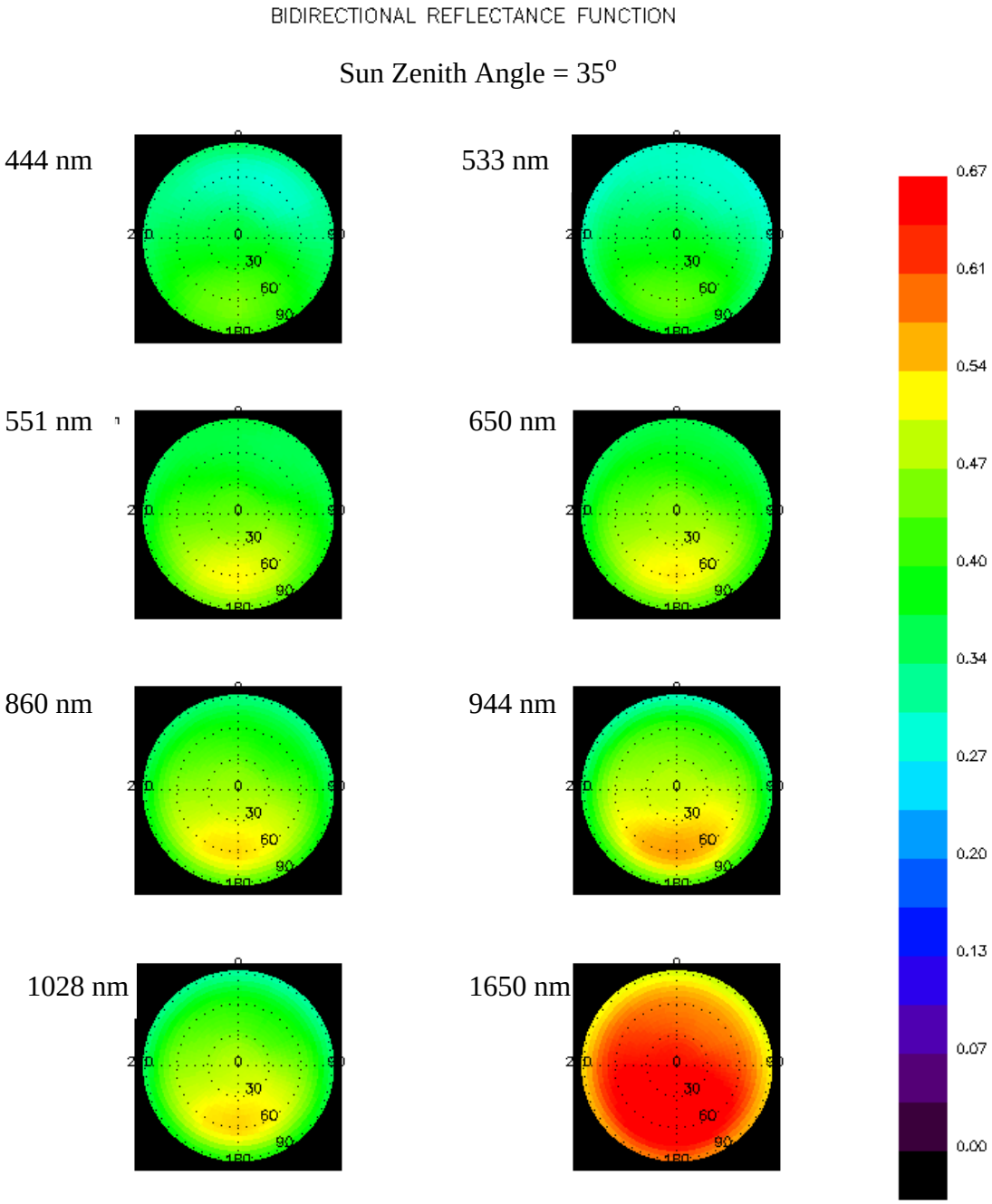
BIDIRECTIONAL REFLECTANCE FUNCTION
Sun Zenith Angle = 35°
444 nm
533 nm
551 nm
650 nm
860 nm
944 nm
1028 nm
1650 nm
0.67
0.61
0.54
0.47
0.40
0.34
0.27
0.20
0.13
0.07
0.00

Figure 2.

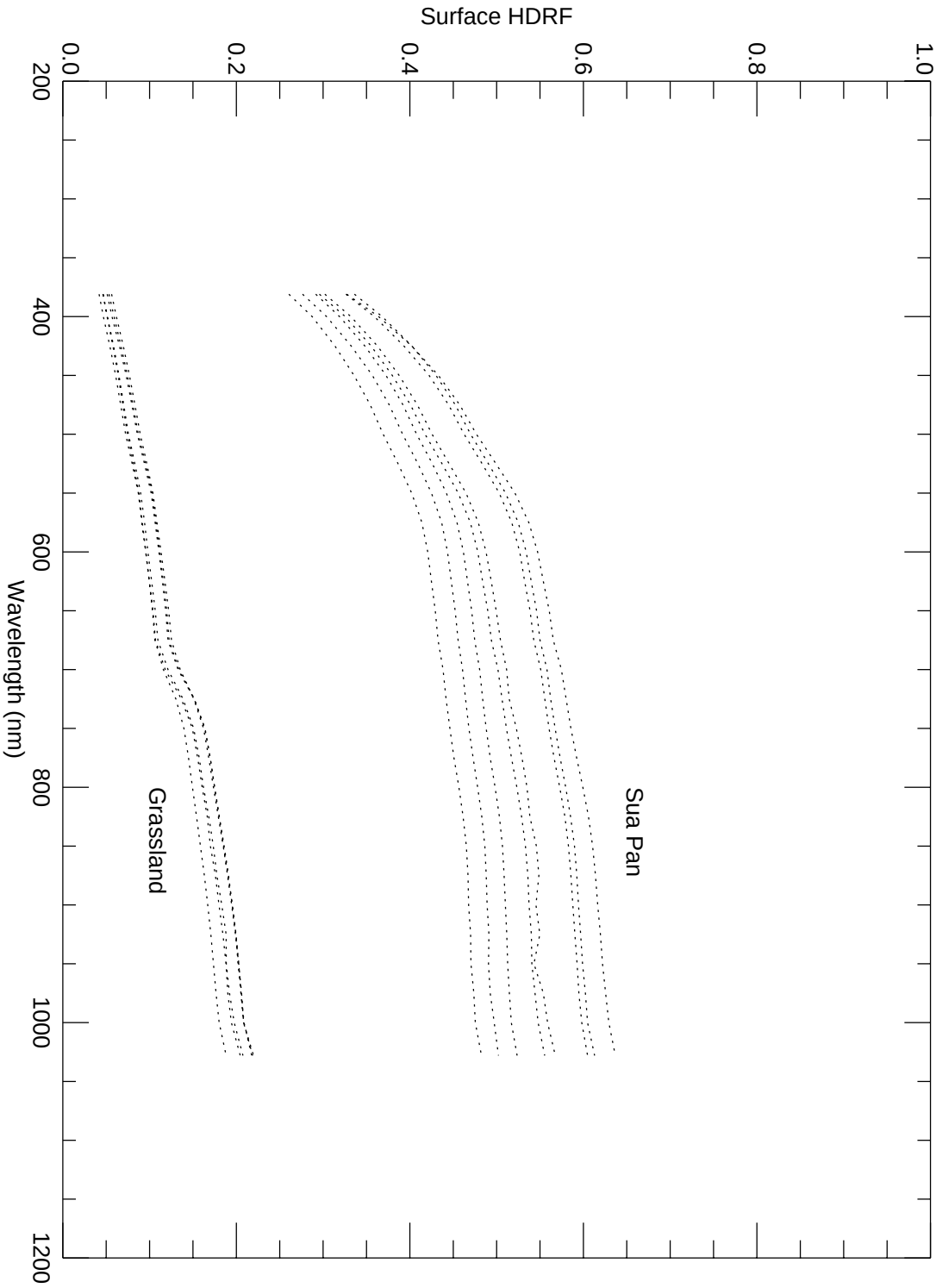
Surface HDRF
0.0
0.2
0.4
0.6
0.8
1.0
200
400
600
800
1000
1200
Wavelength (nm)
Sua Pan
Grassland

Figure 3.

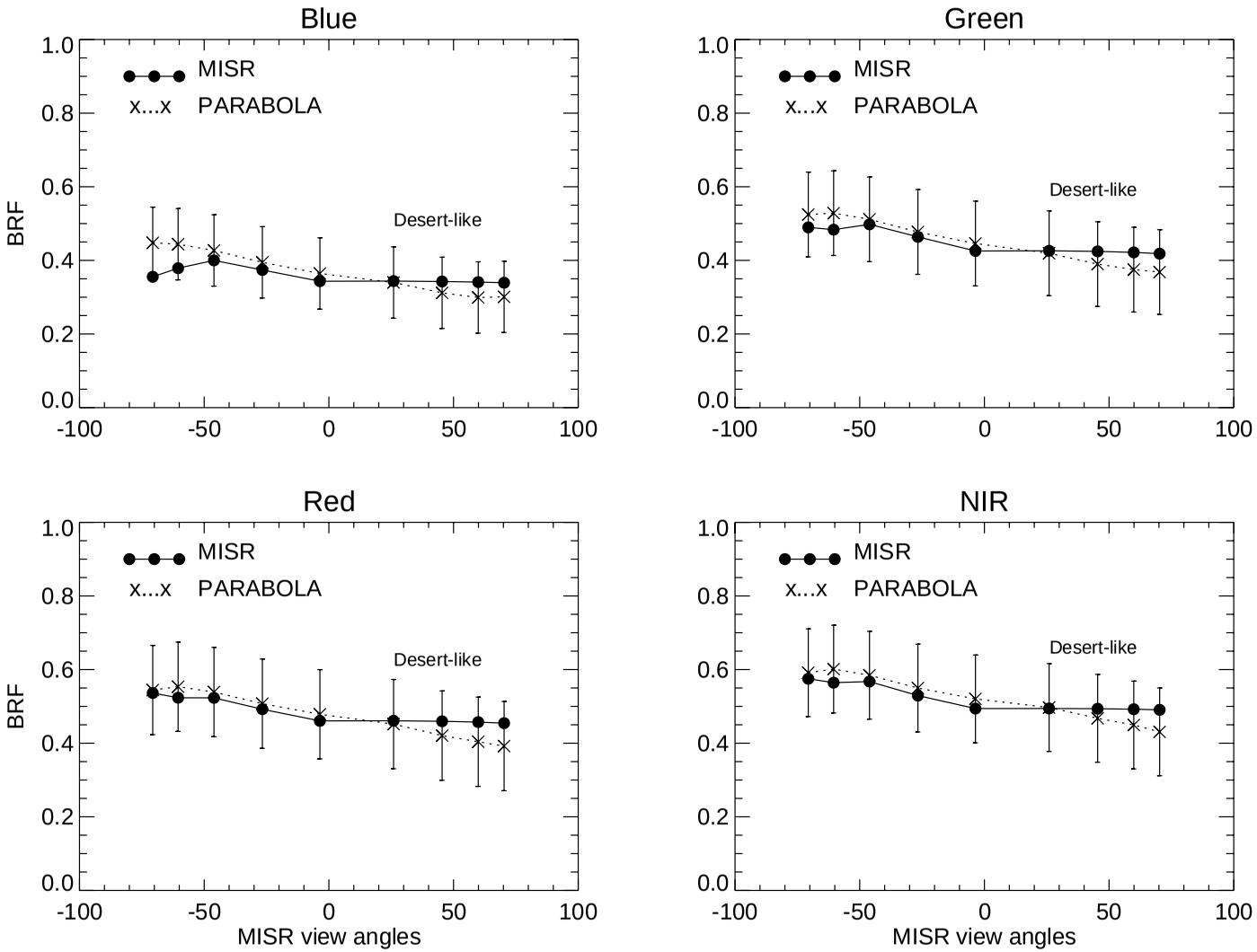
Blue
Green
Red
NIR
MISR
x...x PARABOLA
Desert-like
BRF
MISR view angles
1.0
0.8
0.6
0.4
0.2
0.0
-100
-50
0
50
100

Figure 4.

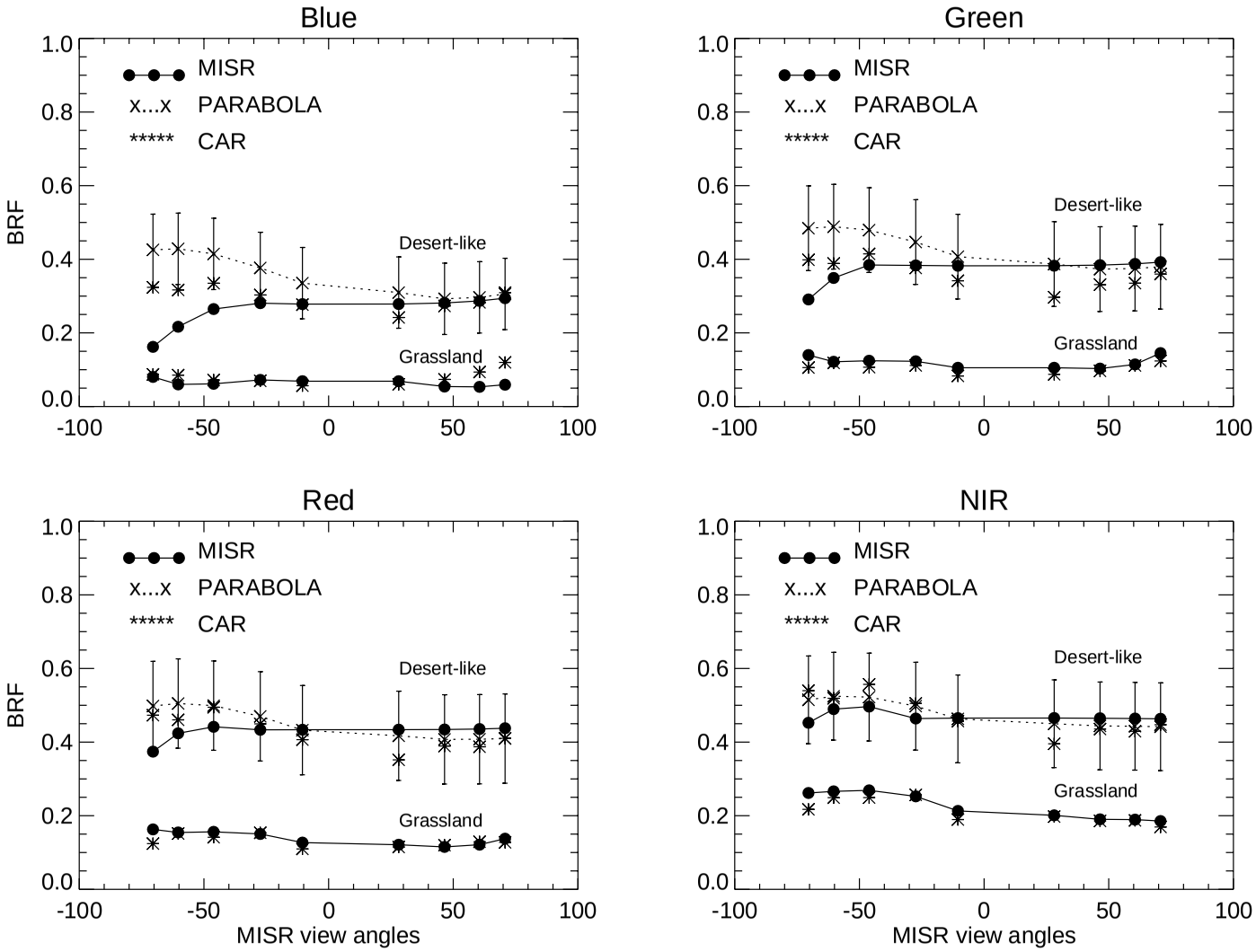
Blue
Green
Red
NIR
MISR
PARABOLA
CAR
Desert-like
Grassland
BRF
MISR view angles
1.0
0.8
0.6
0.4
0.2
0.0
-100
-50
0
50
100

Figure 5.

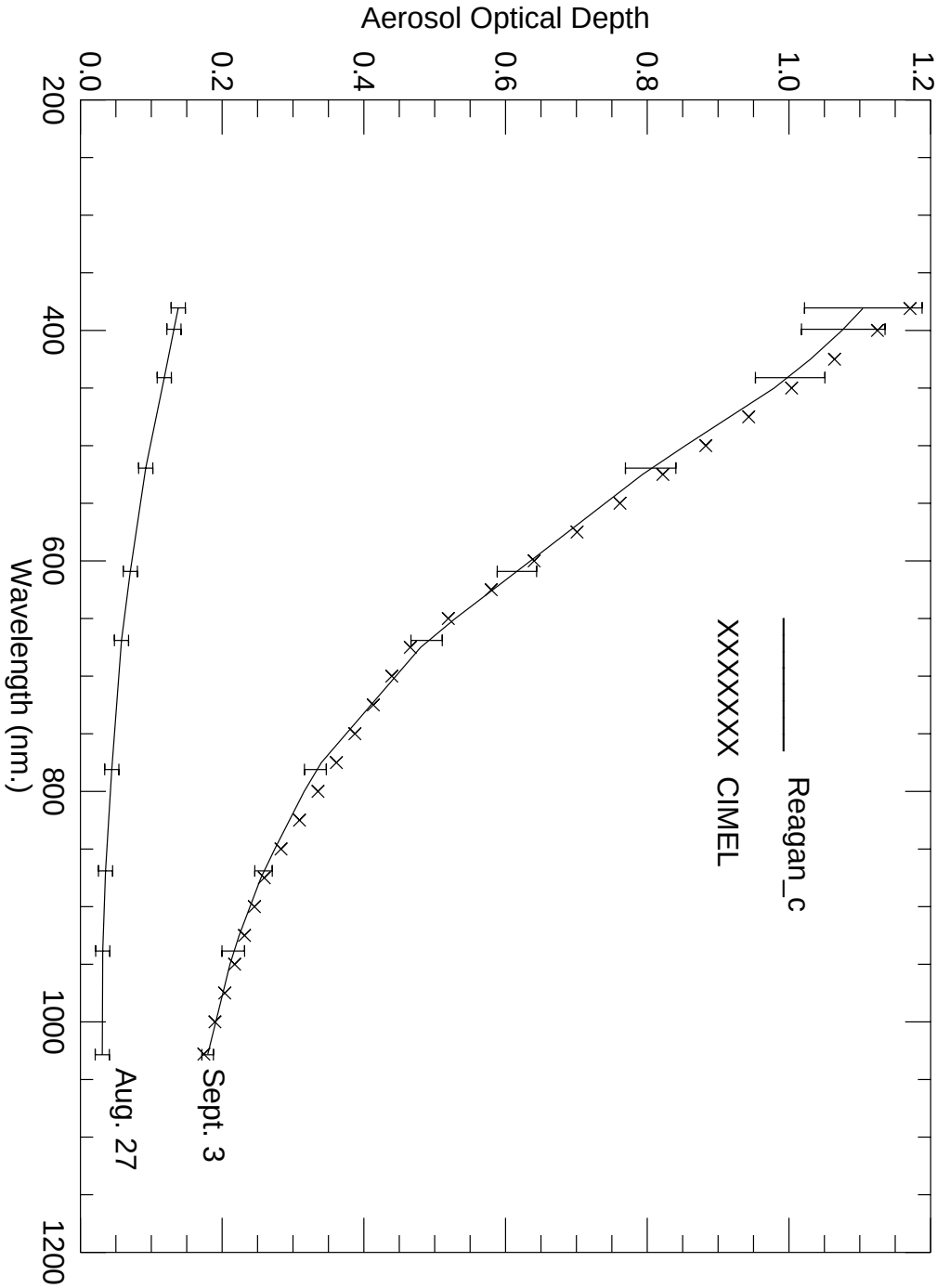
Sua Pan (Safari 2000)
Aerosol Optical Depth
Wavelength (nm.)
Reagan_c
CIMEL
Sept. 3
Aug. 27
0.0
0.2
0.4
0.6
0.8
1.0
1.2
200
400
600
800
1000
1200

Figure 6.

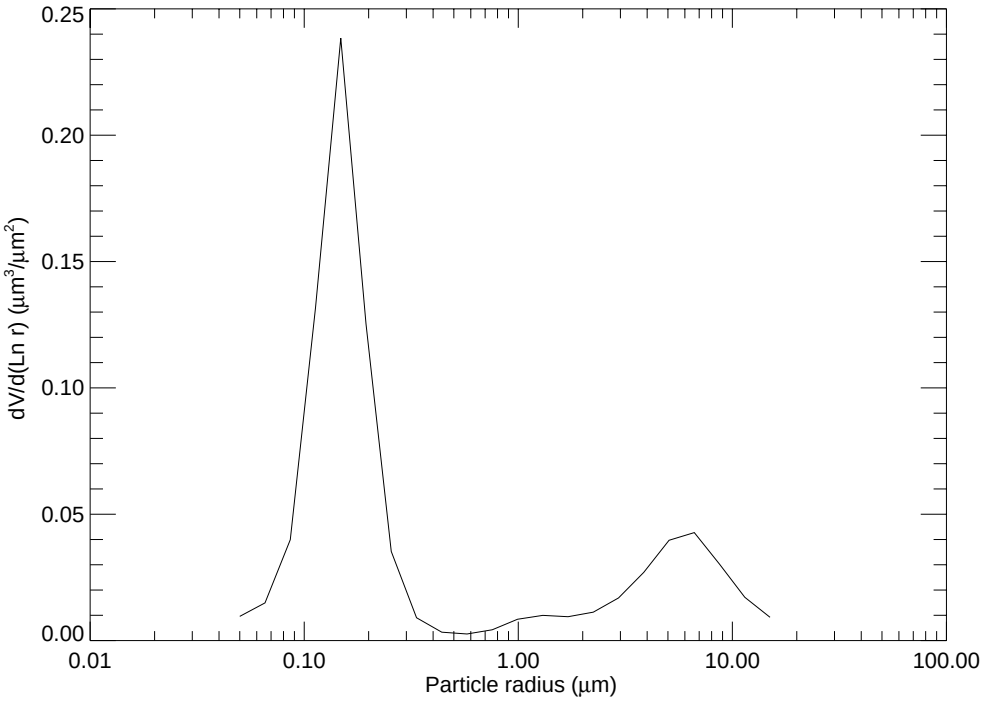

Figure 7a.

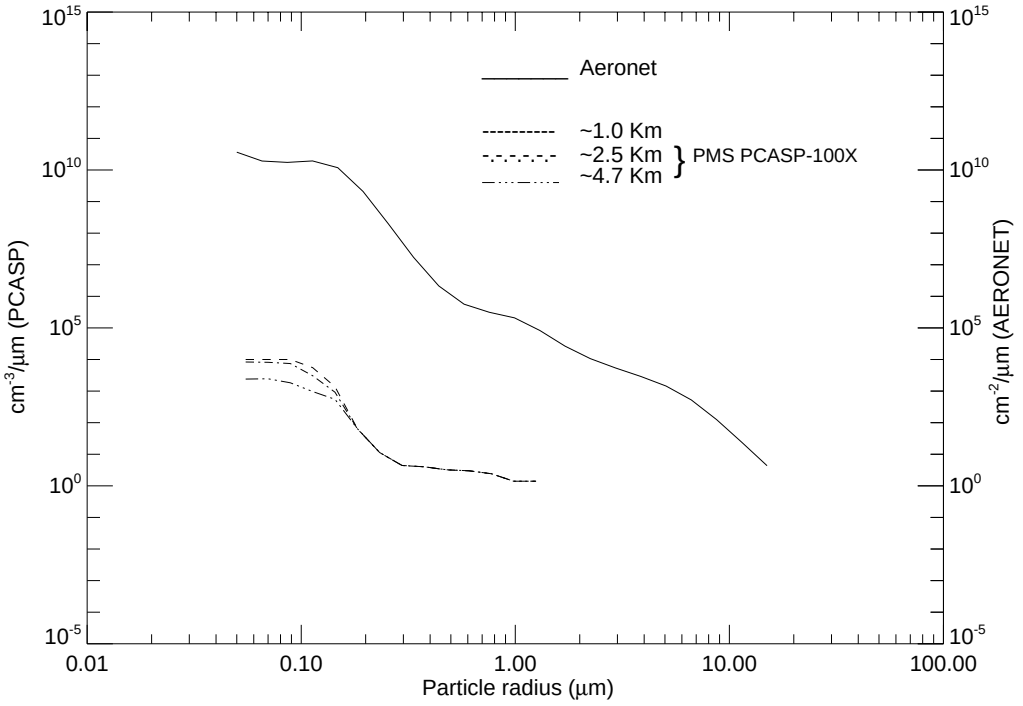

Figure 7b.

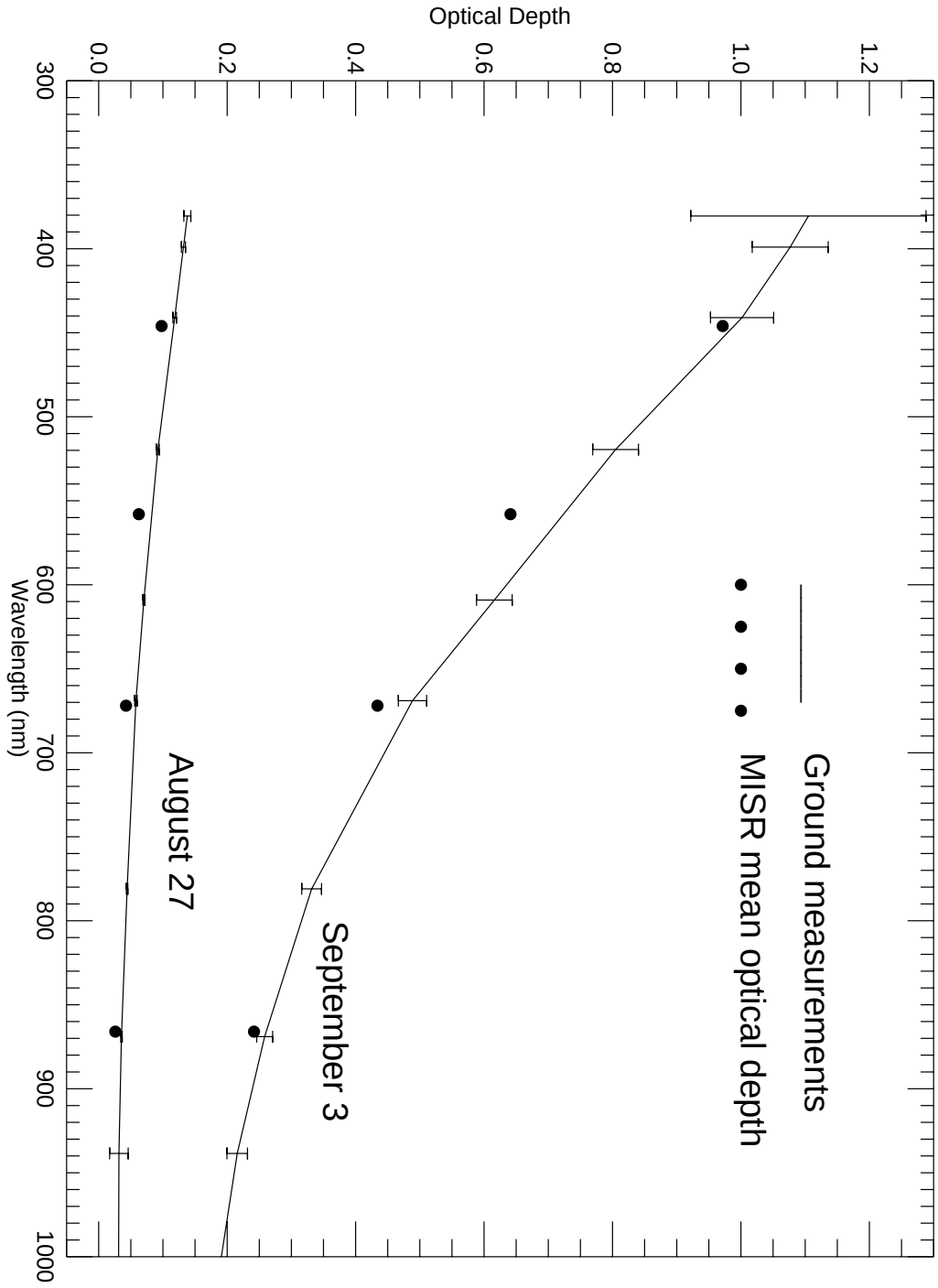
Optical Depth
0.0
0.2
0.4
0.6
0.8
1.0
1.2
300
400
500
600
700
800
900
1000
Wavelength (nm)
Ground measurements
MISR mean optical depth
August 27
September 3

Figure 8.

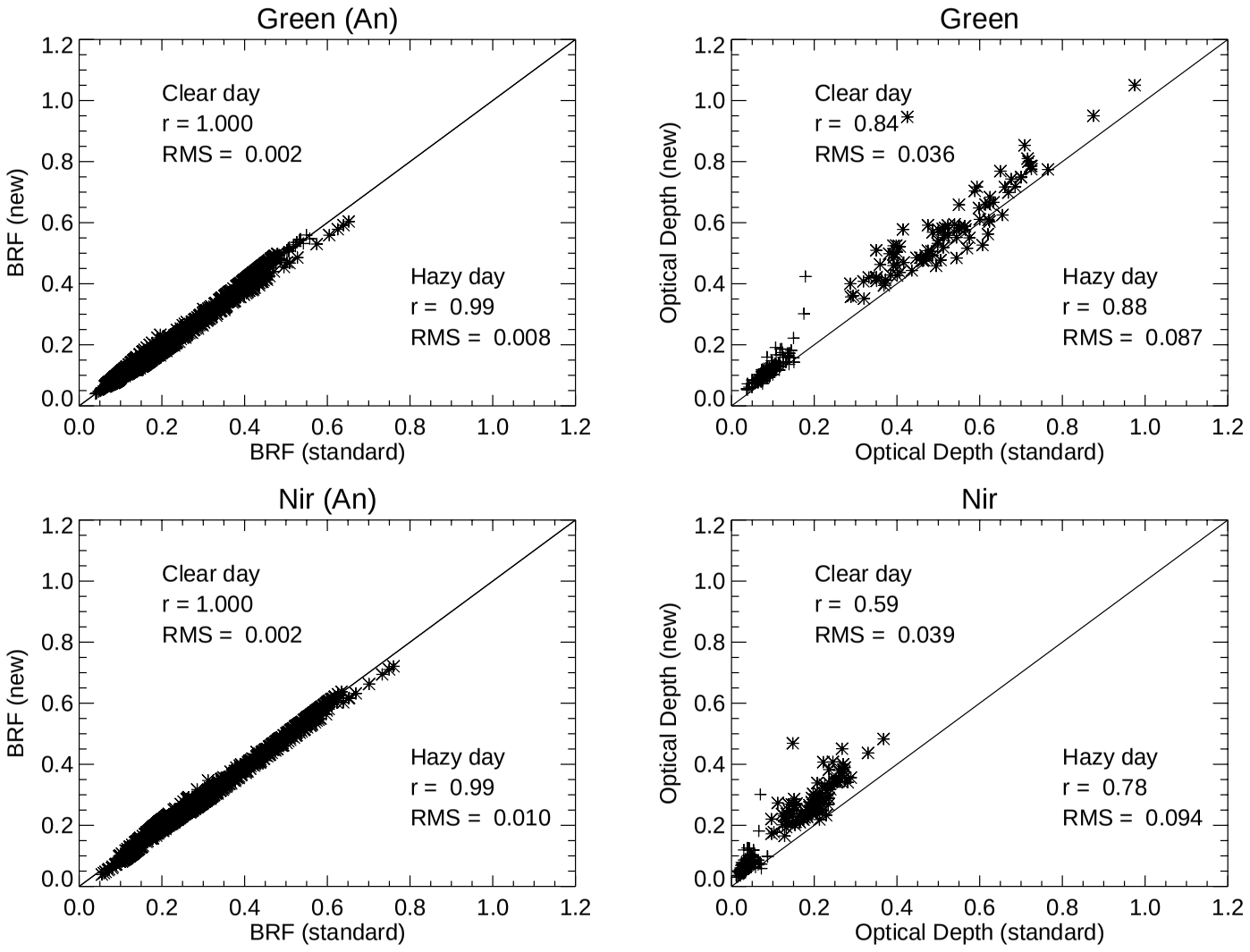
Green (An)
Clear day
r = 1.000
RMS = 0.002
Hazy day
r = 0.99
RMS = 0.008
BRF (new)
BRF (standard)
Green
Clear day
r = 0.84
RMS = 0.036
Hazy day
r = 0.88
RMS = 0.087
Optical Depth (new)
Optical Depth (standard)
Nir (An)
Clear day
r = 1.000
RMS = 0.002
Hazy day
r = 0.99
RMS = 0.010
BRF (new)
BRF (standard)
Nir
Clear day
r = 0.59
RMS = 0.039
Hazy day
r = 0.78
RMS = 0.094
Optical Depth (new)
Optical Depth (standard)

Figure 9.

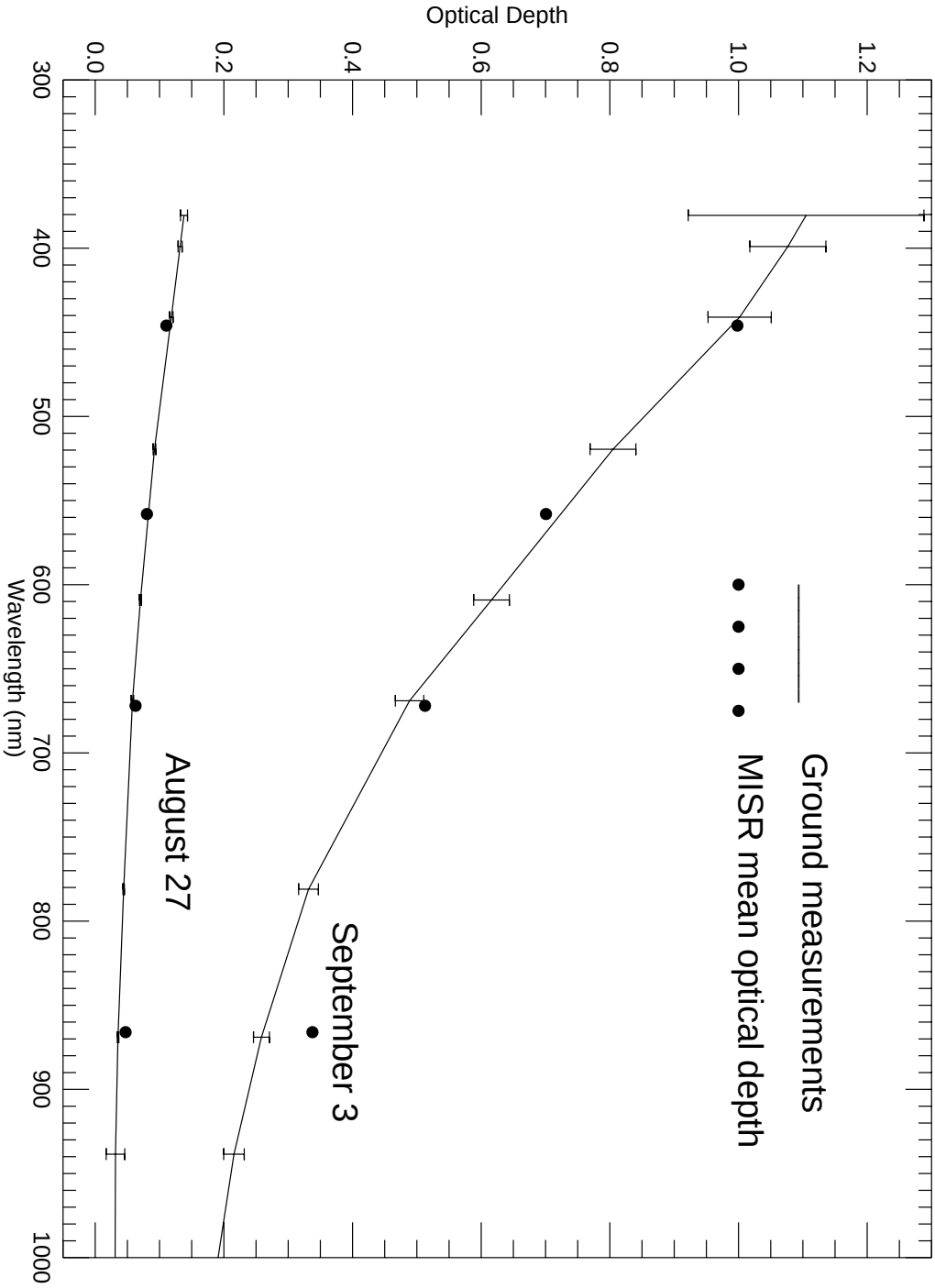
Optical Depth
0.0
0.2
0.4
0.6
0.8
1.0
1.2
300
400
500
600
700
800
900
1000
Wavelength (nm)
Ground measurements
MISR mean optical depth
August 27
September 3

Figure 10.

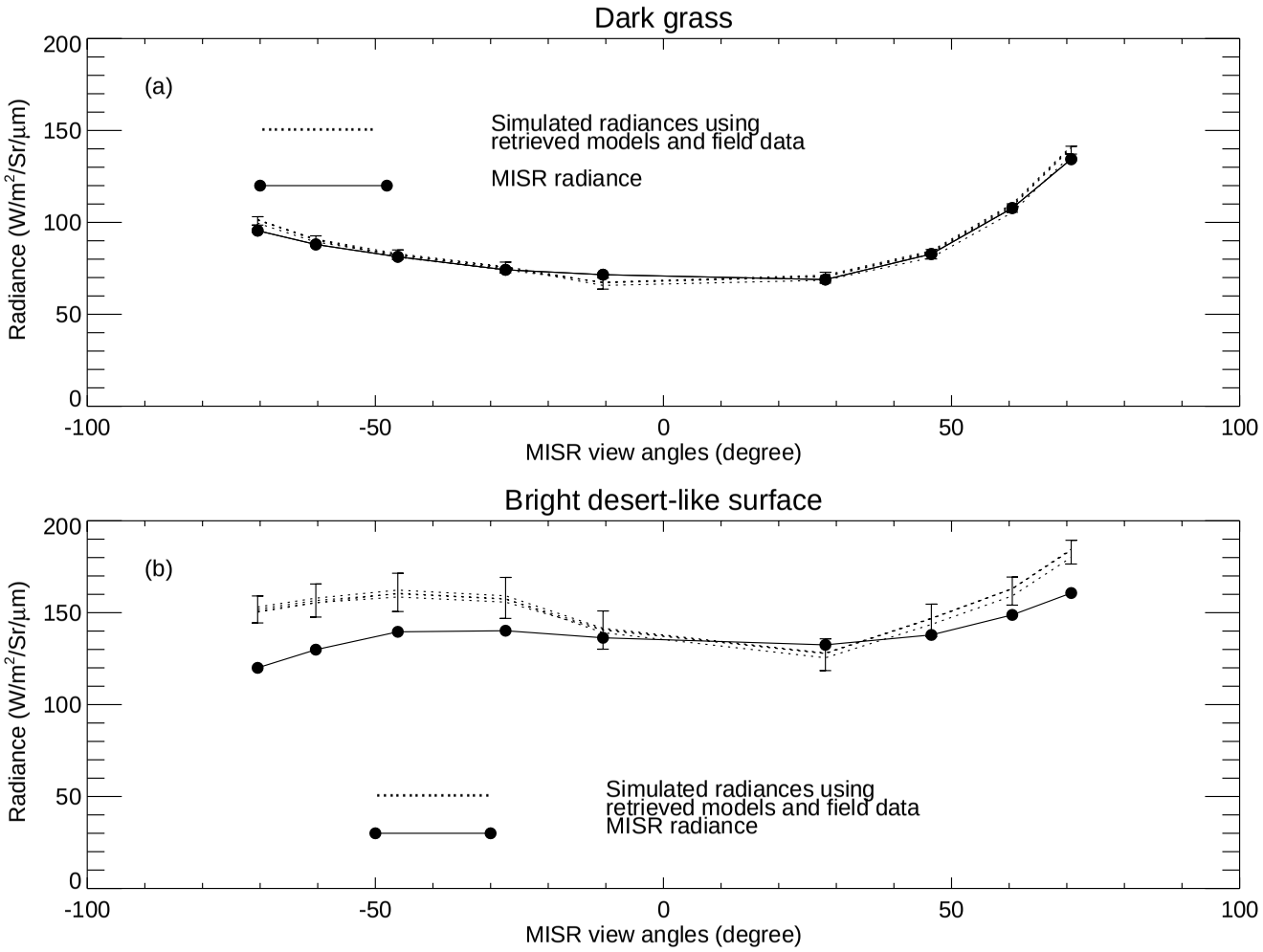
Dark grass
(a)
Simulated radiances using
retrieved models and field data
MISR radiance
Radiance (W/m²/Sr/µm)
MISR view angles (degree)
Bright desert-like surface
(b)
Simulated radiances using
retrieved models and field data
MISR radiance
Radiance (W/m²/Sr/µm)
MISR view angles (degree)

Figure 11.